IOP Publishing Superconductor Science and Technology
Supercond. Sci. Technol. 31 (2018) 055003 (6pp) https://doi.org/10.1088/1361-6668/aab4ea

# Critical current enhancement driven by suppression of superconducting fluctuation in ion-gated ultrathin FeSe

**T Harada[1], J Shiogai[1], T Miyakawa, T Nojima and A Tsukazaki**

Institute for Materials Research, Tohoku University, Sendai 980-8577, Japan

E-mail: t.harada@imr.tohoku.ac.jp

Received 8 December 2017, revised 18 February 2018
Accepted for publication 7 March 2018
Published 28 March 2018

**Abstract**

The framework of phase transition, such as superconducting transition, occasionally depends on the dimensionality of materials. Superconductivity is often weakened in the experimental conditions of two-dimensional thin films due to the fragile superconducting state against defects and interfacial effects. In contrast to this general trend, superconductivity in the thin limit of FeSe exhibits an opposite trend, such as an increase in critical temperature ($T_c$) and the superconducting gap exceeding the bulk values; however, the dominant mechanism is still under debate. Here, we measured thickness-dependent electrical transport properties of the ion-gated FeSe thin films to evaluate the superconducting critical current ($I_c$) in the ultrathin FeSe. Upon systematically decreasing the FeSe thickness by the electrochemical etching technique in the Hall bar-shaped electric double-layer transistors, we observed a dramatic enhancement of $I_c$ reaching about 10 mA and corresponding to about $10^7$ A cm$^{-2}$ in the thinnest condition. By analyzing the transition behavior, we clarify that the suppressed superconducting fluctuation is one of the origins of the large $I_c$ in the ion-gated ultrathin FeSe films. These results indicate the existence of a robust superconducting state possibly with dense Cooper pairs at the thin limit of FeSe.

Supplementary material for this article is available online

Keywords: superconductivity, FeSe, thin films, two-dimensional, critical current, fluctuation, chalcogenide

(Some figures may appear in colour only in the online journal)

## 1. Introduction

Exotic electronic phases have been widely investigated in two-dimensional (2D) layered materials with the advanced experimental techniques of thin film growth, cleaving, and ionic gating [1–5]. Regarding 2D superconductivity in layered materials, the monolayer FeSe on $SrTiO_3$ has attracted keen attention because of the emergence of a high-temperature superconducting phase exhibiting a large superconducting gap far beyond the bulk value [6, 7], which has been intensively explored by scanning tunneling microscopy [8, 9] and angle-resolved photoemission spectroscopy [10–13]. In addition to spectroscopic studies, the electrical transport measurements are beneficial to explore the origin of the high-temperature superconducting phase based on the characterization of the superconducting critical parameters in ultrathin FeSe [8, 14–18]. Up to now, it has been reported that the amorphous-Si/FeTe-capped monolayer FeSe/$SrTiO_3$ shows an onset critical temperature $T_c^{on}$ of about 40 K, critical current density $J_c \sim 1.7 \times 10^6$ A cm$^{-2}$ at 2 K, and an out-of-plane upper critical field $B_{c2}$ exceeding 52 T at 10 K [8]. These are considerably larger than the corresponding values of bulk FeSe ($T_c \sim 8$ K, $J_c \sim 10^4$ A cm$^{-2}$, and $B_{c2} \sim 16.3$ T) [19, 20]. To address the origin of such large critical parameters in the monolayer FeSe, systematic thickness-dependent experiments bridging the bulk and monolayer data are

[1] These authors contributed equally to the work.

 

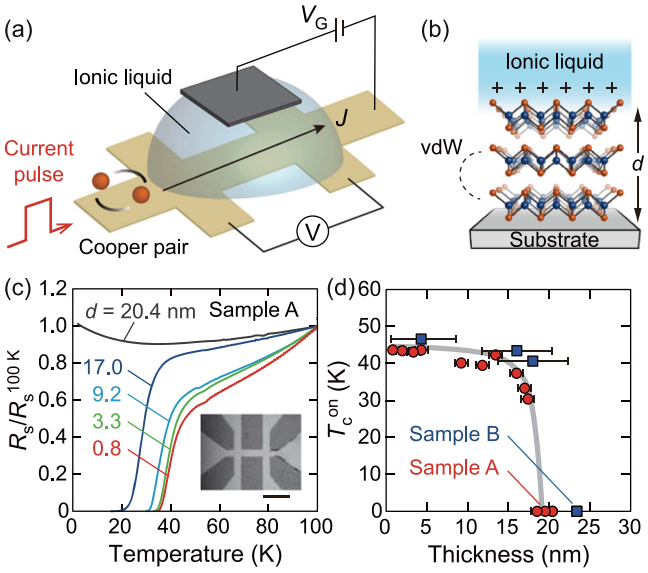


**Figure 1.** Measurement setup and basic characterization. (a) Schematic of measurement configuration with a Hall bar-shaped EDLT. Pulsed current was applied to elucidate the critical current and the BKT transition temperature under the minimal effect of Joule heating. (b) Concept of EDLT. The FeSe thickness $d$ can be reduced by electrochemical etching by ionic liquid at a high temperature of ~250 K. Layered crystal structure of FeSe with van der Waals (vdW) bonding is schematically shown. (c) Temperature dependence of the normalized sheet resistance of sample A at different $d$. The inset shows the optical micrograph of the patterned FeSe Hall bar. The scale bar corresponds to 100 $\mu$m. (d) Thickness dependence of $T_c^{on}$ for samples A (red circles) and B (blue squares).

highly informative. In our previous work, the FeSe thickness dependence of onset $T_c$ has been investigated by electrical transport measurements with an electrochemical etching technique [15]. By applying a gate voltage ($V_G$) of 5 V, an almost constant $T_c^{on} \sim 40$ K has been observed when the sample thickness $d$ is below ~15 nm. In this study, we examine the thickness dependence of two other critical parameters, critical current $I_c$ and critical current density $J_c$, according to the analysis based on the Berezinskii–Kosterlitz–Thouless (BKT) theory [21, 22], which provides insight into the superconducting fluctuation. With decreasing FeSe thickness, the $I_c$ of the FeSe electric double-layer transistor (EDLT) at the lowest measurement temperature is dramatically enhanced by two orders of magnitude from $10^{-4}$ to $10^{-2}$ A. Comparing $T_c^{on}$ and the BKT transition temperature, we argue that the superconducting fluctuation at the 2D limit is anomalously suppressed, indicating that a high superfluid density is realized. We propose that this suppression could be one of the possible origins of the robust high-$T_c$ phase in ultrathin ion-gated FeSe.

## 2. Methods

The current–voltage ($I$–$V$) characteristics and electrical resistance were measured as a function of temperature $T$, magnetic field $B$, and thickness $d$ using an EDLT configuration as depicted in figures 1(a) and (b). We fabricated a well-defined Hall bar device with width $w = 30\,\mu$m and length $l = 80\,\mu$m (figure 1(c), inset) by using a lift-off technique (see supplementary information available online at stacks.iop.org/SUST/31/055003/mmedia) [23] to characterize the wide range of $J_c$ in the order of $10^7$ A cm$^{-2}$. Ionic liquid N,N-diethyl-N-methyl-N-(2-methoxyethyl)ammonium bis(trifluoromethanesulphonyl)imide was selectively put on the Hall bar channel and a gate electrode to apply a gate voltage. Following previous studies [15, 24], the film thickness $d$, which is estimated using the assumption that $d$ is proportional to the temporal integration of the gate leak current, was controlled by using electrochemical etching, which was induced at around 250 K under the gate voltage of 5 V. This assumption was cross-checked with the thickness determined from x-ray diffraction fringes before and after the etching process [15]. To minimize Joule heating, a pulsed excitation current was employed in the $I$–$V$ characteristics to evaluate $I_c$ and the BKT transition temperature. We measured two FeSe EDLT samples with different initial thicknesses: 20.4 nm (sample A), and 23.4 nm (sample B). As shown in the typical temperature dependence of the normalized sheet resistance ($R_s$–$T$) for sample A (figure 1(c)), the initial FeSe with $d = 20.4$ nm shows insulating properties, which is followed by the emergence of a superconducting transition after reducing thickness below $d = 17.0$ nm. This is the consequence of the charge accumulation by the ionic liquid gating and the charge transfer from the $SrTiO_3$ substrate [15, 24]. Such an insulator–superconductor transition in an FeSe thin film has been also reported in experiments using post annealing, which changes the carrier concentration in the sample [17]. The $T_c^{on}$ increases with decreasing $d$, reaching 43 K below $d = 15$ nm for both samples A and B (figure 1(d)).

## 3. Results and discussion

### 3.1. *I–V characteristics*

Figures 2(a)–(f) show the $I$–$V$ characteristics for sample A and sample B, respectively, at different thickness conditions: (a) $d = 17.0 \pm 0.8$, (b) $3.3 \pm 0.8$, and (c) $0.8 \pm 0.8$ nm for sample A; (d) $d = 18.0 \pm 4.3$, (e) $16.0 \pm 4.3$, and (f) $4.3 \pm 4.3$ nm for sample B. The $I$–$V$ characteristics were linear above $T_c^{on}$, which corresponds to the ohmic resistance in the normal state. In contrast, they become considerably nonlinear below $T_c^{on}$, and then show the zero voltage regions with further decreasing temperature, implying the emergence of superconductivity with the finite critical current $I_c$. The fast rise of voltage reaching the order of 10 mV just above $I_c$ as shown in figures 2(a)–(f) is related to the high normal-state resistance of several hundred ohms of the FeSe channel. The notable feature is that the critical current $I_c$ dramatically increases despite the decrease in the FeSe channel thickness ((a) to (c) and (d) to (f)). Considering the constant $V_G = 5$ V applied with the same channel width and length, we can systematically discuss $I_c$ as the thickness-dependent quantity in both FeSe EDLT devices, although the current flow may not be uniform along the thickness direction. This unusual $I_c$

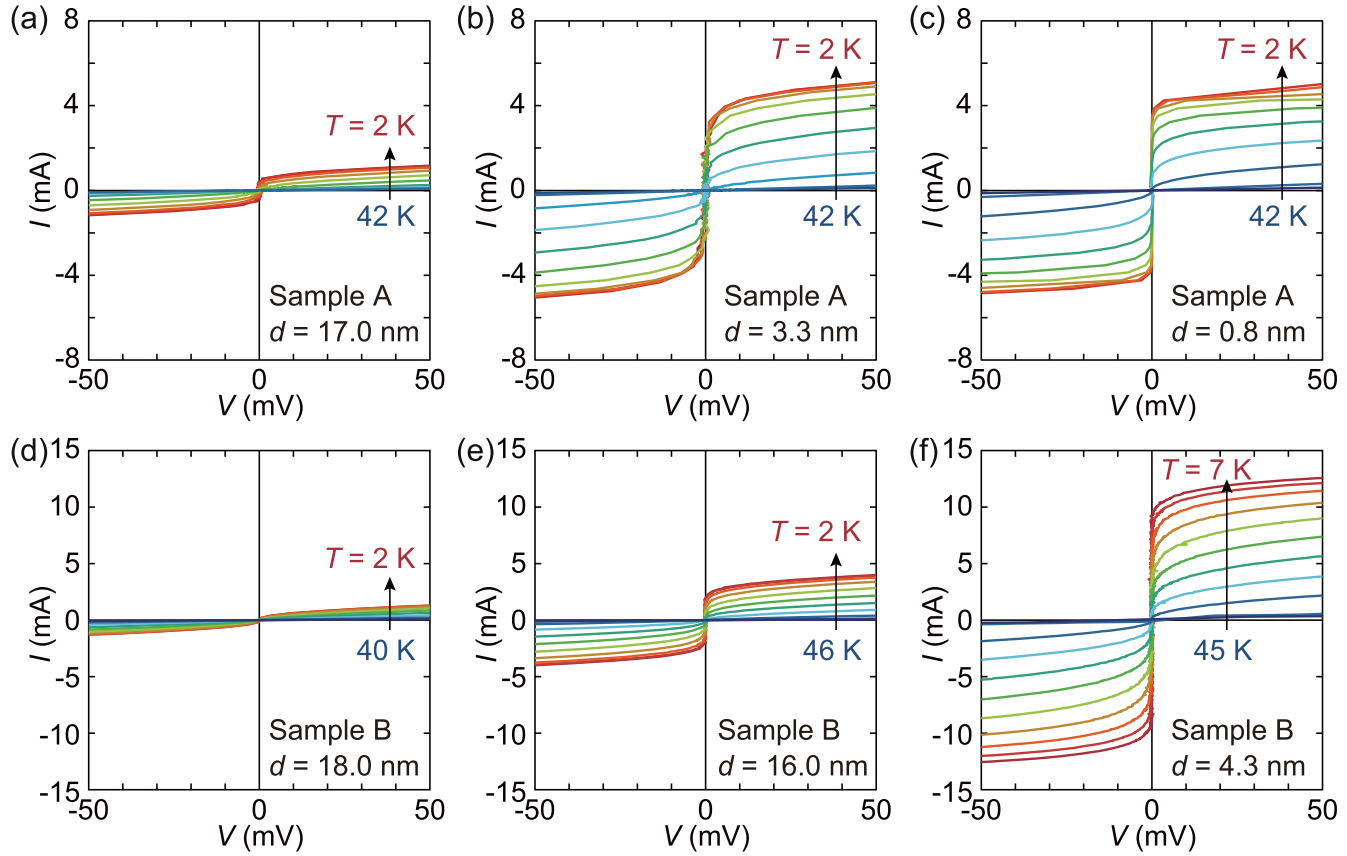


**Figure 2.** *I*–*V* characteristics of the FeSe EDLTs with varied thickness. (a)–(c) Temperature-dependent *I*–*V* characteristics for sample A at (a) $d = 17.0$ nm, (b) 3.3 nm, and (c) 0.8 nm. (d)–(f) Those for sample B at (d) $d = 18.0$ nm, (e) 16.0 nm, and (f) 4.3 nm.

enhancement with the reduction of conducting channel thickness could reflect the enhancement of 2D superconductivity in the FeSe EDLT.

Here, we note that our definition of the $I_c$ is the current generating $10^{-4}$ V for sample A and $10^{-3}$ V for sample B. Such relatively high voltage criteria were employed due to the large noise originating from the high series resistance at the thick FeSe channels outside the ionic liquid in our sample configuration, which have the same thickness as those at the initial condition. However, the high voltage criteria do not significantly alter our discussion focusing on $I_c$ at the lowest measurement temperature, owing to the steep log*V*–log*I* behavior with the five orders of magnitude change of *V* as shown in figures 3(a) and (b). If the simple extrapolation of log*V*–log*I* curves is valid, the $I_c$ value is hardly affected even when we change the cutoff voltage criterion to the widely-used $10^{-6}$ V. The thickness dependences of $I_c$ for sample A and sample B are summarized in figure 3(d). The inset shows an abrupt increase of $I_c$ by one order of magnitude around $d = 15$ nm. Below $d \sim 15$ nm, the high $I_c$ exceeding 1 mA further increases with decreasing *d* for both samples. The connection among the increase of $I_c$, the characteristic temperatures of $T_c^{on}$, and the BKT transition is discussed below.

### *3.2. The BKT transition and fluctuation*

Next, we discuss the superconducting fluctuation, which can be evaluated by comparing the $T_c^{on}$ and zero-resistance temperature. Since the dimensionality of superconductivity in a bulk FeSe is still under debate as discussed in the supplementary information, we carefully adopt the BKT analysis to examine the dimensionality of the FeSe EDLT for all thickness conditions. The *I*–*V* characteristics shown in figures 2(c) and (f) are replotted logarithmically in figures 3(a) and (b) for sample A with $d = 0.8$ nm and sample B with $d = 4.3$ nm, respectively. All the log*I*–log*V* data obey the BKT-like power law $V \propto I^{\alpha}$ at low current, as is consistent with the literature [8, 25, 26]. Upon decreasing the temperature, the exponent $\alpha$ abruptly increases, as shown in figure 3(c). According to the BKT theory, the crossing point of the $\alpha - T$ curve and $\alpha = 3$ line corresponds to the BKT transition temperature ($T_{BKT}^{IV}$), below which the zero ohmic resistance state emerges in the $I \to 0$ limit because the vortices are bound in vortex–anti-vortex pairs. In addition to the $\alpha - T$ curves, we confirmed that the Halperin–Nelson formula fits the $R_S$–$T$ curve well (supplementary data), indicating that the transport property in the thin FeSe EDLT is governed by the BKT transition. Unexpectedly, the superconducting transition in the thick FeSe EDLT satisfies the BKT criteria even for the thickness exceeding the bulk coherence length of ~3 nm. Such a behavior has also been observed in a rather thick 500 nm FeSe film, with an indication of the quasi-2D nature of superconductivity [25]. From the above discussion, we employ the $T_{BKT}^{IV}$ as the zero-resistance temperature.

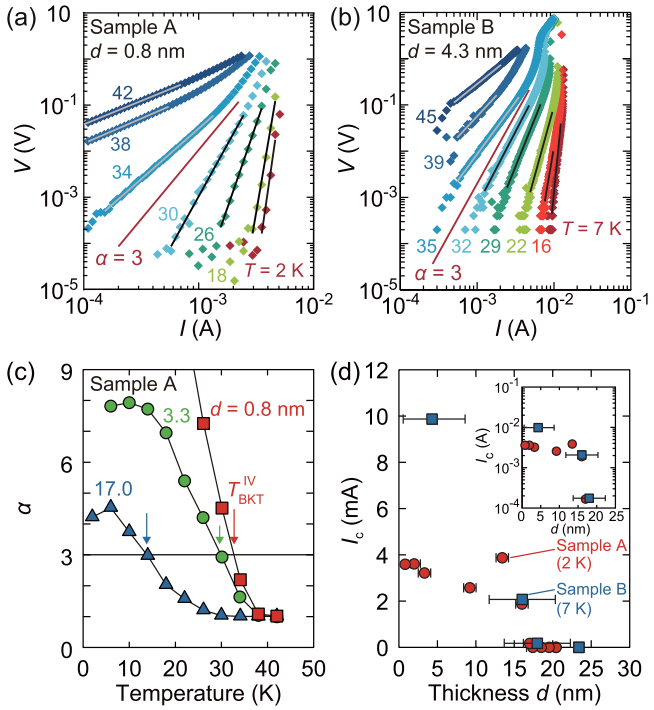


**Figure 3.** *I*–*V* characteristics plotted in logarithmic scale (a) for sample A at $d = 0.8$ nm, and (b) for sample B at $d = 4.3$ nm. The slopes of black and gray lines give the power law exponent $\alpha$. The red line denotes the relation of $V \propto I^3$. (c) Temperature dependence of the exponent $\alpha$ obtained from Log*I*–Log*V* plot for sample A at various thicknesses. (d) The thickness dependence of $I_c$ for sample A (red circles) at 2 K and sample B (blue squares) at 7 K plotted in linear and logarithmic (inset) scales.

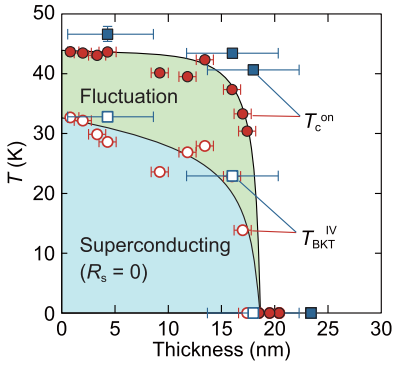


**Figure 4.** Thickness dependences of $T_{BKT}{}^{IV}$ (open symbols) and $T_c{}^{on}$ (filled symbols) for samples A (red circles) and B (blue squares). The FeSe EDLTs are in the superconducting state with zero ohmic resistance in the light blue region, while the finite resistance appears due to superconducting fluctuation in the light green region.

We plot $T_{BKT}{}^{IV}$ as a function of $d$ together with $T_c{}^{on}$ in figure 4. In both samples A (red circles) and B (blue squares), $T_{BKT}{}^{IV}$ keeps increasing as FeSe thickness decreases, while the $T_c{}^{on}$ almost saturates below $d = 15$ nm. Since $I_c$ scales well with $T_{BKT}{}^{IV}$ below $d = 15$ nm (supplementary data), we suppose that the $I_c$ enhancement shown in figure 3(d) is driven by the increase of $T_{BKT}{}^{IV}$, not $T_c{}^{on}$. The temperature region between $T_c{}^{on}$ and $T_{BKT}{}^{IV}$ highlighted with green corresponds to the superconducting transition region, where the amplitude and/or phase of the superconducting order parameter are fluctuated. Here, we speculate the possible supercurrent distribution in the FeSe EDLT in certain thickness conditions because it is likely that there are three regions with different amplitudes of superconducting order parameter in the FeSe EDLT: the top EDL/FeSe, the middle bulk-like FeSe, and the bottom FeSe/$SrTiO_3$. Superconductivity in the thickest conditions above 15 nm is rather fragile because of the low $T_c{}^{on}$ and the strong fluctuation evidenced by the broad transition. This could indicate that the current flow is not uniform due to the coexistence of a thin superconducting region and thick normal state in FeSe, which originates from the EDLT configuration where electrons are accumulated both at the top and at the bottom of the FeSe layer by ionic liquid gating and charge transfer from the $SrTiO_3$ substrate [24]. In the medium thickness conditions of about 5∼15 nm, high $T_c{}^{on}$ is obtained, but the transition is still strongly fluctuated. Considering the previous results on thickness-dependent Hall measurements [24], we believe that the current uniformity starts to be established in this condition. In the thinnest condition below ∼5 nm, the wave functions of electrons at the top and bottom of the FeSe layer are overlapped, forming electron-rich regions over a length scale of a few nm [24]. This can lead to a rather uniform superconductivity with the high $T_c{}^{on}$ and sharp transition, where the order parameter well expands to the whole thickness region. Since the superconducting state is homogeneous in the whole film at $d = 0.8$ nm, we can safely calculate the critical current density as $J_c = I_c/dw$, which is as high as $1.5 \times 10^7$ A cm$^{-2}$ at 2 K for sample A. This value is in the order of 30% of the depairing current density $J_{depair} \sim 5.2 \times 10^7$ A cm$^{-2}$ (supplementary data). The sharpest transition and the large $J_c$ at the thinnest condition is quite unusual because this opposes the general trend in the fragile 2D superconductivity.

### 3.3. Estimation of superfluid density

Finally, we propose two possible enhancement factors for the large $I_c$ and $J_c$ at the ultrathin limit in FeSe EDLT, focusing only on the homogeneous thinnest thickness condition. The first is the enhancement of superfluid density at zero temperature $n_{s0}$, which is evaluated by the London penetration depth based on $T_{BKT}{}^{IV}$ (supplementary data). With decreasing FeSe thickness, $n_{s0}$ monotonically increases. The value of $n_{s0}$ has a clear correlation with the Hall coefficient $R_H$ in the normal state, indicating that the electron charge accumulation is contributing to the enhanced $n_{s0}$ in the ultrathin FeSe EDLT (supplementary data). The calculated $n_{s0} \sim 6.7 \times 10^{20}$ cm$^{-3}$ at the thinnest condition (sample A, $d = 0.8$ nm) is higher than that for the 1 ML FeSe $\sim 4.4 \times 10^{20}$ cm$^{-3}$ grown by molecular beam epitaxy, which is obtained by applying the same analysis to the reported data [8], and is possibly due to the charge accumulation by ion gating. When the same evaluation scheme is applied to the thicker conditions in spite of the current flow possibly not being uniform, we clearly obtain a positive correlation between the $J_c$ and the $n_{s0}$ (supplementary data). This trend indicates that the suppression of the superconducting fluctuation due to increased $n_{s0}$ is the origin of the enhanced $J_c$ in the thinnest FeSe EDLT. We note that

the calculated $n_{s0}$ value for the 1ML FeSe is one order smaller than that measured by muon spin damping $\sim 6 \times 10^{21}\,\mathrm{cm}^{-3}$ [27]. The underestimation of $n_{s0}$ in our analysis would be due to the use of an oversimplified model. Nevertheless, the increase in $n_{s0}$ along the thickness reduction and its correlation with $J_c$ are worth further investigation; for instance, by using other measurement techniques such as the mutual inductance method [28] to reveal the origin of the enhanced $J_c$ in the ultrathin FeSe EDLTs. Since the highest $J_c$ observed in the thin limit is still lower than the estimated $J_{depair}$, we may consider the pinning effect of vortices induced by the self-field as the origin of high $J_c$. We note that the increase in $n_{s0}$ also results in the enhancement of the pinning potential as well as the suppression of superconducting fluctuation, assuming that the pinning sites, which are possibly located around the FeSe/substrate interface, are unchanged with thickness in the thin region. Elucidating the pinning centers in the superconductors at 2D limit would be another important issue for future research. The second possible factor for the largest $I_c$ at the thin limit could be the 2D layered crystal structure. Interestingly, as another example of the enhancement in robustness, $TaS_2$ has been reported to show the higher critical temperature and larger critical current with decreasing thickness [29], although the enhanced $J_c$ ($\sim 5 \times 10^5\,\mathrm{A\,cm}^{-2}$) of $TaS_2$ is much lower than that of the ion-gated FeSe. Both FeSe and $TaS_2$ have the a common layered crystal structure with the conducting layers weakly bonded by van der Waals interactions (figure 1(b)). Such a specific 2D crystal structure might also play a role in maintaining a robust superconducting state even in the ultrathin condition.

## 4. Conclusion

We have systematically measured the thickness dependence of the electrical transport properties of FeSe in the EDLT configuration. In addition to the previously reported $T_c^{on}$ enhancement, we revealed $I_c$ enhancement with thickness reduction toward the ultrathin regime. By detailed analysis of the transition behavior, we conclude that the superconducting fluctuation is well suppressed because of an increase of superfluid density at the thinnest condition, which is unusual behavior compared with the general trend in 2D superconductivity. Our findings prove that the combination of two-dimensionality and high superfluid density plays a key role for the robust superconductivity in ion-gated FeSe.

## Acknowledgments

The authors thank T Seki and K Takanashi for help in the cleanroom facility through a cooperative program (No. 16G0404) of the CRDAM-IMR, and K Fujiwara and J Mannhart for valuable discussions. This work is partly supported by the Grant-in-Aid for Specially Promoted Research (No. KAKENHI 25000003), for Challenging Exploratory Research (No. KAKENHI 15K13354), and for Research Activity Start-up (15H06029), from the Japan Society for the Promotion of Science.

## ORCID iDs

T Harada https://orcid.org/0000-0002-8657-2258

## References

[1] Novoselov K S, Geim A K, Morozov S V, Jiang D, Katsnelson M I, Grigorieva I V, Dubonos S V and Firsov A A 2005 Two-dimensional gas of massless Dirac fermions in graphene *Nature* **438** 197–200
[2] Zhang Y, Tan Y-W, Stormer H L and Kim P 2005 Experimental observation of the quantum Hall effect and Berry's phase in graphene *Nature* **438** 201–4
[3] Wang Q-Y *et al* 2012 Interface-induced high-temperature superconductivity in single unit-cell FeSe films on $SrTiO_3$ *Chin. Phys. Lett.* **29** 037402
[4] Xi X, Zhao L, Wang Z, Berger H, Forró L, Shan J and Mak K F 2015 Strongly enhanced charge-density-wave order in monolayer $NbSe_2$ *Nat. Nanotech.* **10** 765–9
[5] Saito Y, Nojima T and Iwasa Y 2016 Highly crystalline 2D superconductors *Nat. Rev. Mater.* **2** 16094
[6] Wang Z, Liu C, Liu Y and Wang J 2017 High-temperature superconductivity in one-unit-cell FeSe films *J. Phys.: Condens. Mater.* **29** 153001
[7] Zhang W *et al* 2014 Interface charge doping effects on superconductivity of single-unit-cell FeSe films on $SrTiO_3$ substrates *Phys. Rev.* B **89** 060506
[8] Zhang W-H *et al* 2014 Direct observation of high-temperature superconductivity in one-unit-cell FeSe films *Chin. Phys. Lett.* **31** 017401
[9] Fan Q *et al* 2015 Plain s-wave superconductivity in single-layer FeSe on $SrTiO_3$ probed by scanning tunnelling microscopy *Nat. Phys.* **11** 946–52
[10] He S *et al* 2013 Phase diagram and electronic indication of high-temperature superconductivity at 65 K in single-layer FeSe films *Nat. Mater.* **12** 605–10
[11] Liu D *et al* 2012 Electronic origin of high-temperature superconductivity in single-layer FeSe superconductor *Nat. Commun.* **3** 931
[12] Lee J J *et al* 2014 Interfacial mode coupling as the origin of the enhancement of $T_c$ in FeSe films on $SrTiO_3$ *Nature* **515** 245–8
[13] He J *et al* 2014 Electronic evidence of an insulator–superconductor crossover in single-layer FeSe/$SrTiO_3$ films *Proc. Natl. Acad. Sci. USA* **111** 18501–6
[14] Ge J-F, Liu Z-L, Liu C, Gao C-L, Qian D, Xue Q-K, Liu Y and Jia J-F 2015 Superconductivity above 100 K in single-layer FeSe films on doped $SrTiO_3$ *Nat. Mater.* **14** 285–9
[15] Shiogai J, Ito Y, Mitsuhashi T, Nojima T and Tsukazaki A 2016 Electric-field-induced superconductivity in electrochemically etched ultrathin FeSe films on $SrTiO_3$ and MgO *Nat. Phys.* **12** 42–6
[16] Sun Y *et al* 2014 High temperature superconducting FeSe films on $SrTiO_3$ substrates *Sci. Rep.* **4** 6040
[17] Wang Q *et al* 2015 Thickness dependence of superconductivity and superconductor-insulator transition in ultrathin FeSe films on $SrTiO_3$ (001) substrate *2D Mater* **2** 044012
[18] Wang Q *et al* 2017 Spin fluctuation induced linear magnetoresistance in ultrathin superconducting FeSe films *2D Mater* **4** 034004

[19] Hsu F-C *et al* 2008 Superconductivity in the PbO-type structure $\alpha$-FeSe *Proc. Natl. Acad. Sci. USA* **105** 14262–4
[20] Lei H, Hu R and Petrovic C 2011 Critical fields, thermally activated transport, and critical current density of $\alpha$-FeSe single crystals *Phys. Rev.* B **84** 014520
[21] Berezinskii V L 1972 Destruction of long-range order in one-dimensional and two-dimensional systems possessing a continuous symmetry group: II. Quantum systems *Sov. Phys. JETP* **34** 610–6
[22] Kosterlitz J M and Thouless D J 1972 Long range order and metastability in two dimensional solids and superfluids *J. Phys.* C **5** L124–6
[23] Harada T and Tsukazaki A 2017 A versatile patterning process based on easily soluble sacrificial bilayers *AIP Adv.* **7** 085011
[24] Shiogai J, Miyakawa T, Ito Y, Nojima T and Tsukazaki A 2017 Unified trend of superconducting transition temperature versus Hall coefficient for ultrathin FeSe films prepared on different oxide substrates *Phys. Rev.* B **95** 115101
[25] Schneider R, Zaitsev A G, Fuchs D and von Löhneysen H 2014 Excess conductivity and Berezinskii–Kosterlitz–Thouless transition in superconducting FeSe thin films *J. Phys. Condens. Matter* **26** 455701
[26] Xing Y *et al* 2015 Quantum Griffiths singularity of superconductor-metal transition in Ga thin films *Science* **350** 542
[27] Biswas P K S, Salman Z, Song Q, Peng R, Zhang J, Shu L, Feng D L, Prokscha T, Suter A and Morenzoni E 2016 Direct evidence of nodeless clean superconductivity and determination of the superfluid density in single-layer FeSe grown on $SrTiO_3$ arXiv:1602.02580
[28] Božović I, He X and Bollinger A T 2016 Dependence of the critical temperature in overdoped copper oxides on superfluid density *Nature* **536** 309–3011
[29] Navarro-Moratalla E *et al* 2016 Enhanced superconductivity in atomically thin $TaS_2$ *Nat. Commun.* **7** 11043